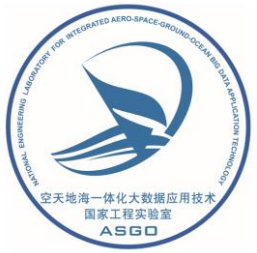

Revisiting Geometric Methods for 3D Point Cloud Registration

Jiaqi Yang（杨佳琪）

Northwestern Polytechnical University

(西北工业大学)

2022.06

Contents

1. Introduction a) Problem definition

- Estimating the 6-DoF (3-DoF Rotation, 3-DoF Translation) pose to align to point clouds

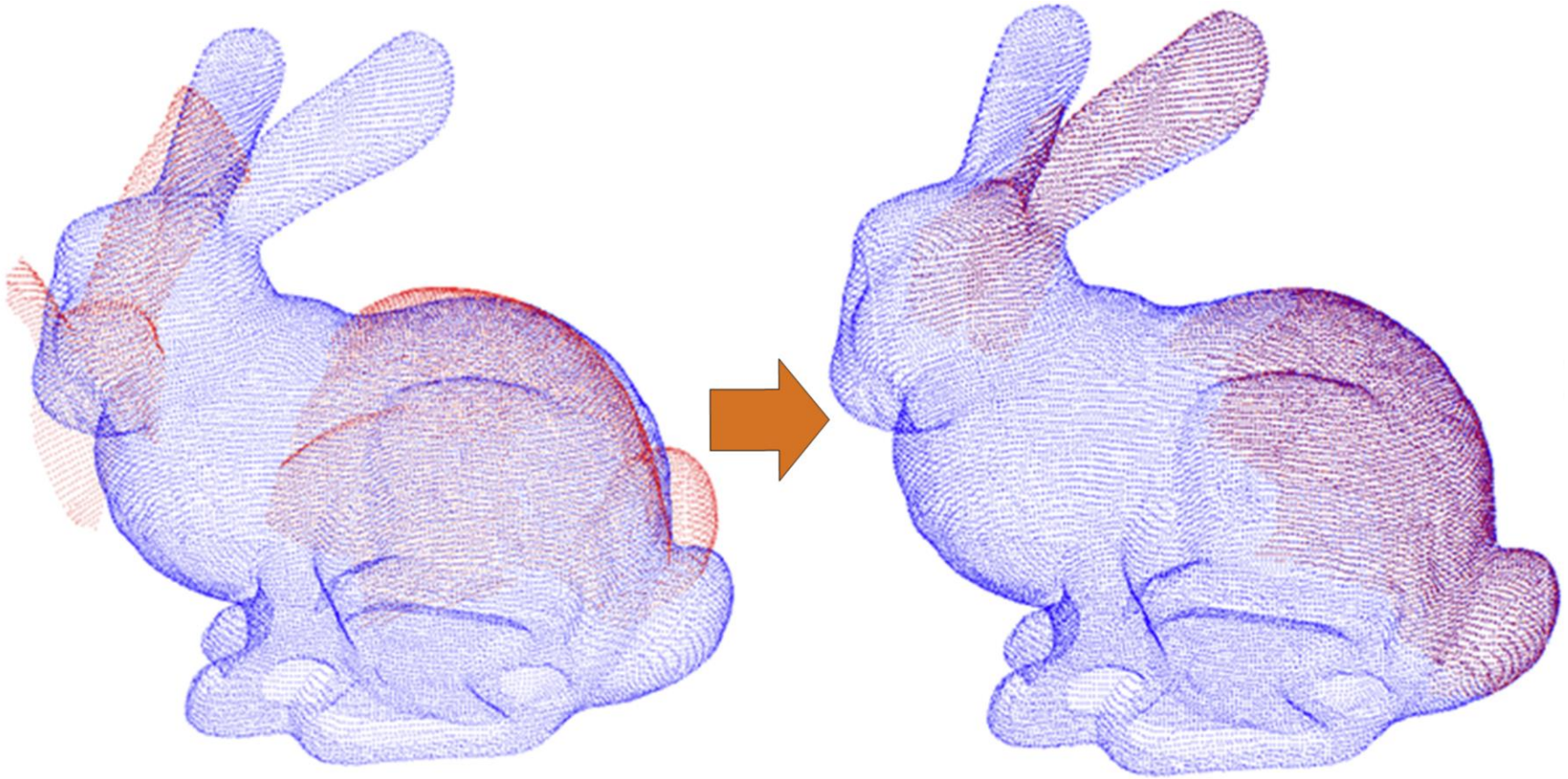

1. Introduction b) Popular solutions

- Learning-based: Learning correspondences/6-DoF Pose from massive training data

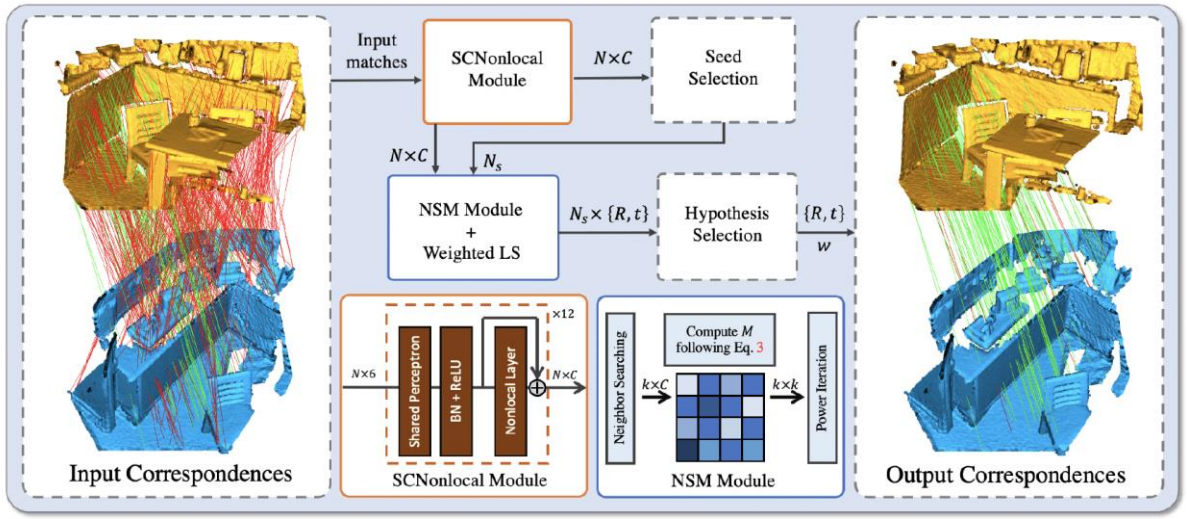

PointDSC 2021

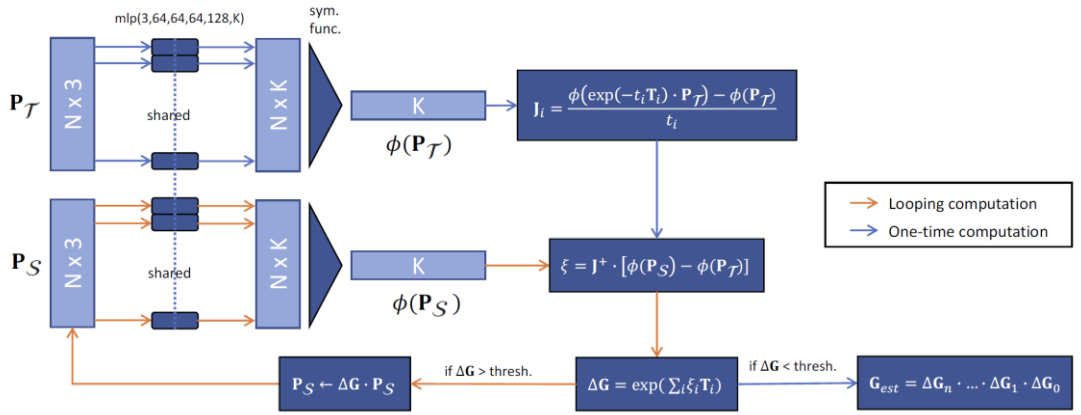

PointNetLK 2019

- **Generalization issue**
- **Training data issue**
- **Label issue**

1. Introduction b) Popular solutions

- Geometry-based: ICP-based, correspondence-based, BnB-based, etc.

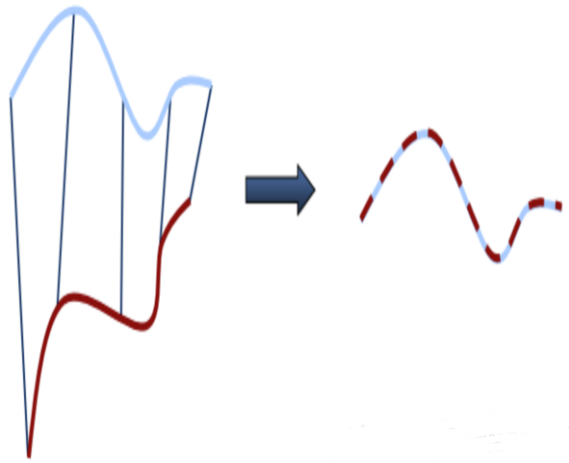

ICP-based

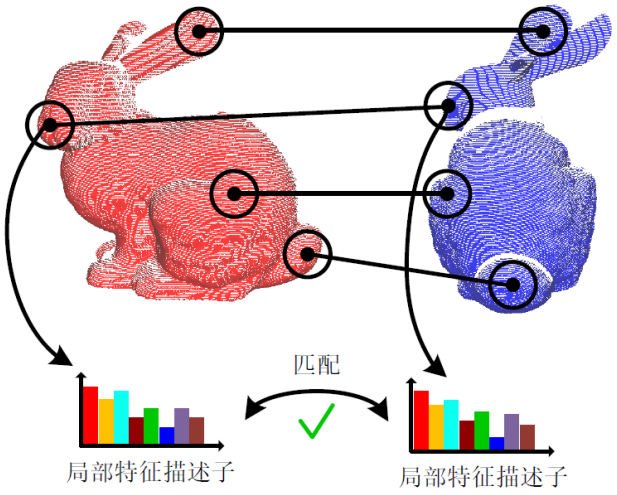

Correspondence-based

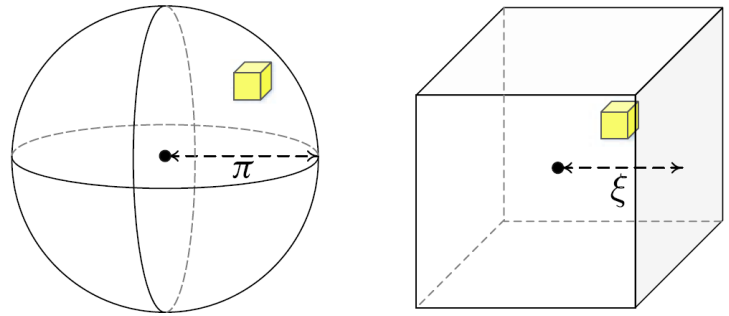

BnB-based

- **Better explainability**
- **No training data requirement**
- **"Green"**

1. Introduction c) our focus

☐ Focus: Correspondence-based with RANSAC

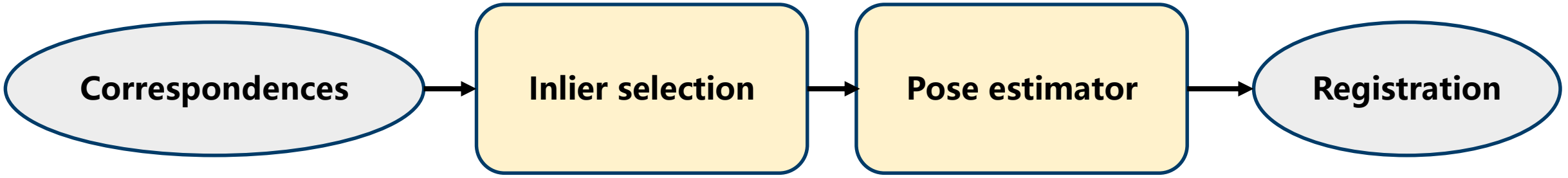

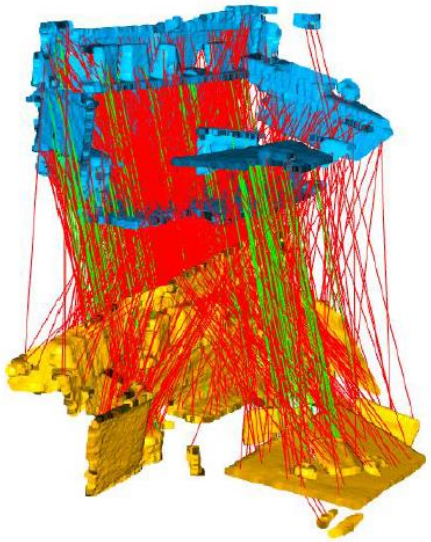

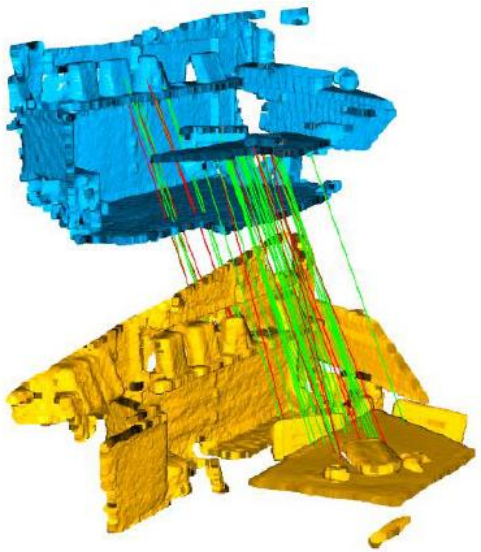

$$\mathbf{R} \in SO(3)$$
$$\mathbf{t} \in \mathbb{R}^3$$

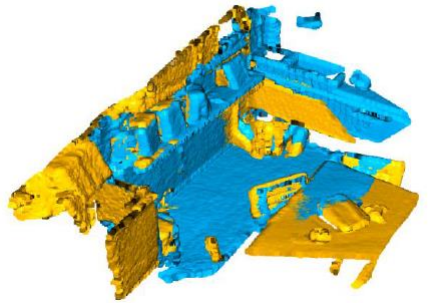

2. Our works a) Feature Matching (LT-GV)

☐ Evaluation (PAMI 2021): the variety of geometric methods

Figure 2: Schematics of the entities involved in local (left) and global (right) voting. Left: local voters are collected in the spherical neighborhood of a correspondence (dark yellow circle). The invariant pairwise compatibility v_L is the minimum ratio of the light red distances. Right: global voters, from which c_2 is sampled, are located arbitrarily (dark yellow). The hypothesized transformation T (solid arrow) gives in this case an inaccurate alignment (dashed arrow) of p_2 (light yellow). The covariant compatibility v_G uses the dark red distance between the hypothesized point and the assigned point p'_2.

CVPR 2013, In search of inliers

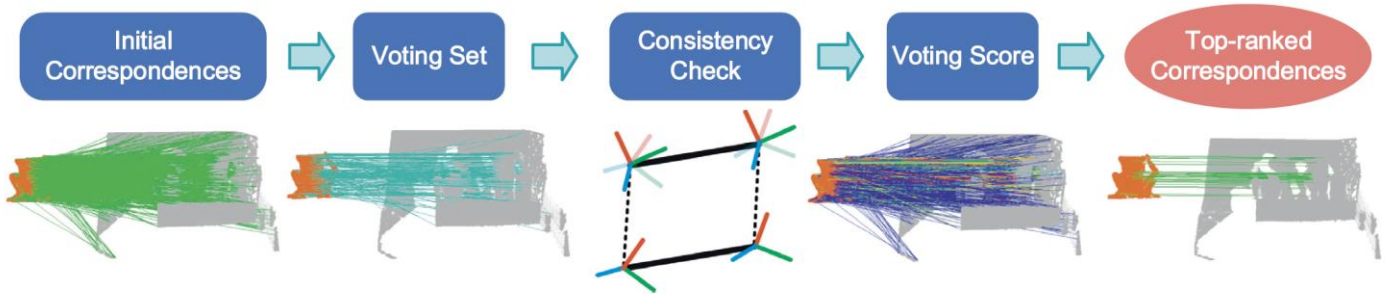

Fig. 1. Pipeline of our CV method. It takes the raw feature matches between the source shape and the target shape as the input, and then assigns a score to each correspondence through checking the consistency of every correspondence with respect to those in a predefined voting set. Finally, initial correspondences are listed in a descending order by the voting score, and top-ranked correspondences can be selected (the number of selected correspondences depends on the application scenario) from the re-ranked correspondence set.

PRL, Consistency voting

Individual-based

2. Our works a) Feature Matching

☐ Evaluation (PAMI 2021): the variety of geometric methods

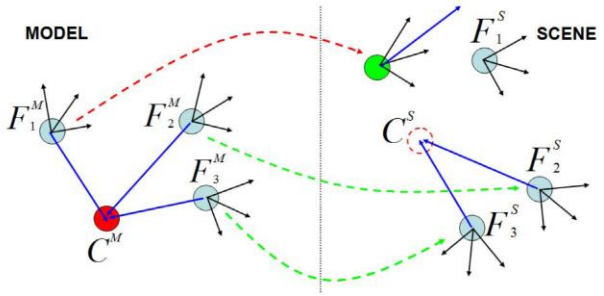

Figure 2. Example of 3D Hough Voting based on local RFs.

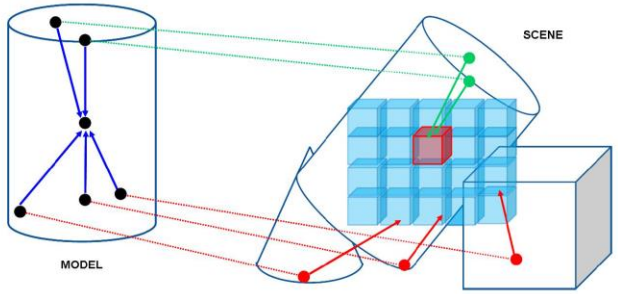

Figure 3. Toy example showing the proposed 3D Hough Voting scheme.

PRSIVT 2010, 3D Hough voting

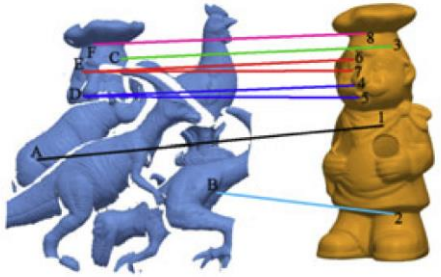

	A1	B2	C3	D4	D5	E6	E7	F8
A1	0	0.12	0.77	0.83	0.98	0.77	0.66	0.75
B2	0.12	0	0.05	0.21	0.37	0.07	0.32	0.17
C3	0.77	0.05	0	0.99	0.6	0.99	0.99	0.7
D4	0.83	0.21	0.99	0	0	0.99	0.99	0.96
D5	0.98	0.37	0.6	0	0	0.9	0.88	0.69
E6	0.77	0.07	0.99	0.99	0.9	0	0	0.98
E7	0.66	0.32	0.99	0.99	0.88	0	0	0.99
F8	0.75	0.17	0.7	0.96	0.69	0.98	0.99	0

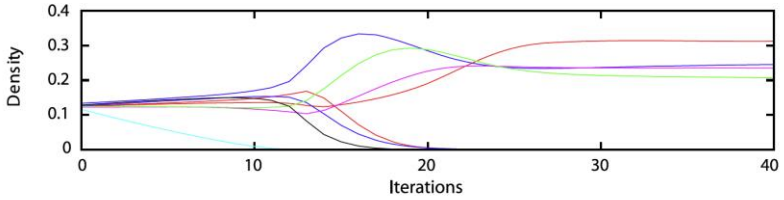

$$\mathbf{x}_i(t+1) = \mathbf{x}_i(t)\frac{(\Pi\mathbf{x}(t))_i}{\mathbf{x}(t)^T\Pi\mathbf{x}(t)}$$

IJCV 2013, Game theory matching

Group-based

2. Our works a) Feature Matching (LT-GV)

☐ LT-GV (TGRS 2022): Loose-Tight Geometric Voting

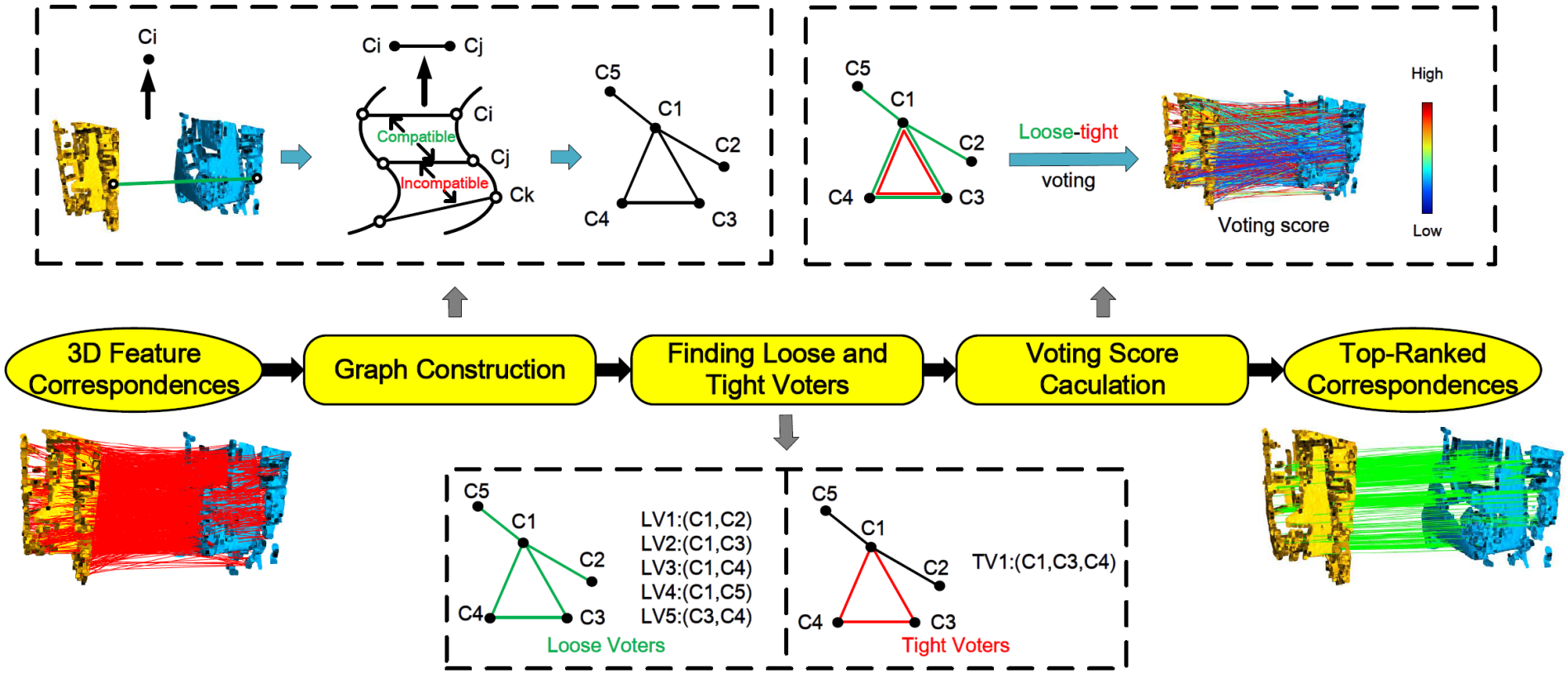

Fig. 1. Pipeline of the proposed method. First, it takes the initial 3D feature correspondences as the input and computes the compatibility scores of each correspondence with others to build a compatibility graph. Then, loose and tight voters are defined in the graph for each correspondence. Finally, the confidence score of a correspondence is assigned based on the voting scores of both loose and tight voters. By ordering correspondences based on their voting scores, consistent correspondences can be efficiently retrieved.

2. Our works a) Feature Matching (LT-GV)

☐ LT-GV : The definition of voters

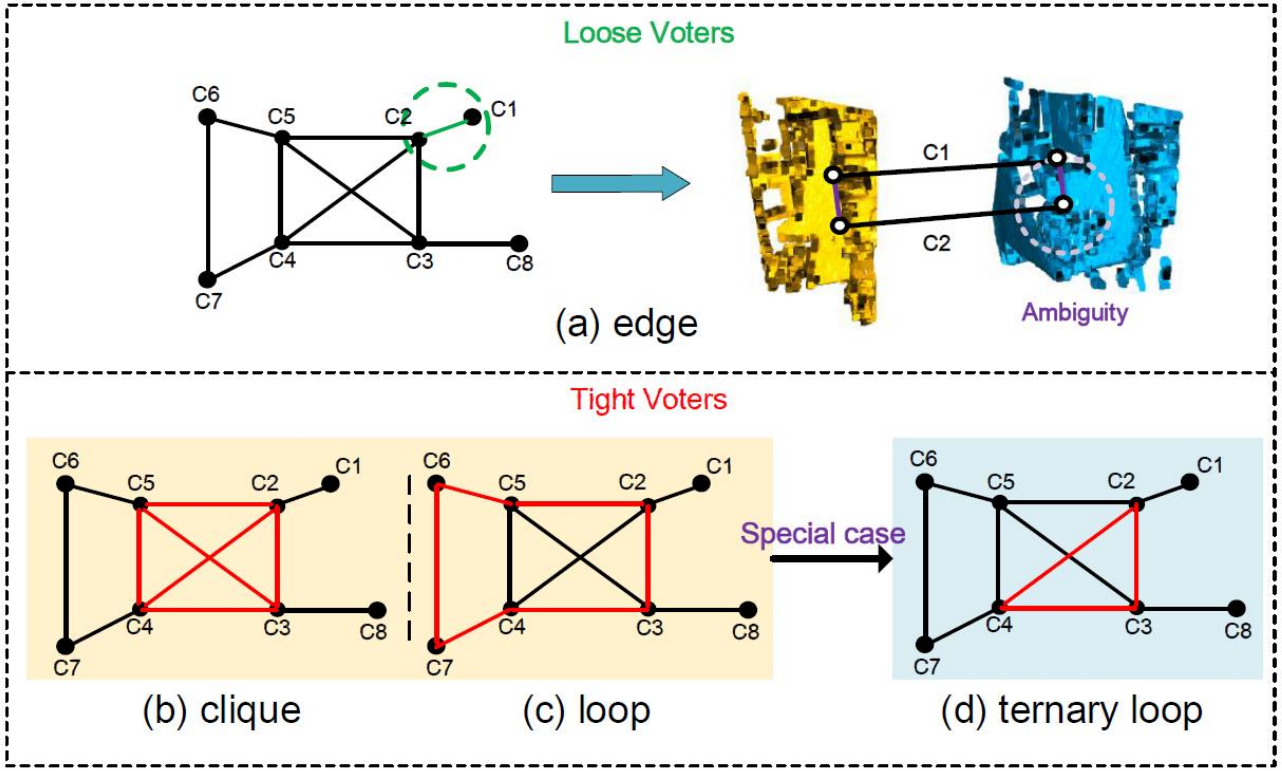

Fig. 2. Illustration of loose and tight voters. (a) Loose voters as graph edges, which are robust yet suffer from ambiguities. From (b) to (d), potential tight voters. Finally, we employ graph edges as loose voters and ternary loops as tight voters. Please refer to the text for specific motivations.

2. Our works a) Feature Matching (LT-GV)

☐ Performance: Feature matching

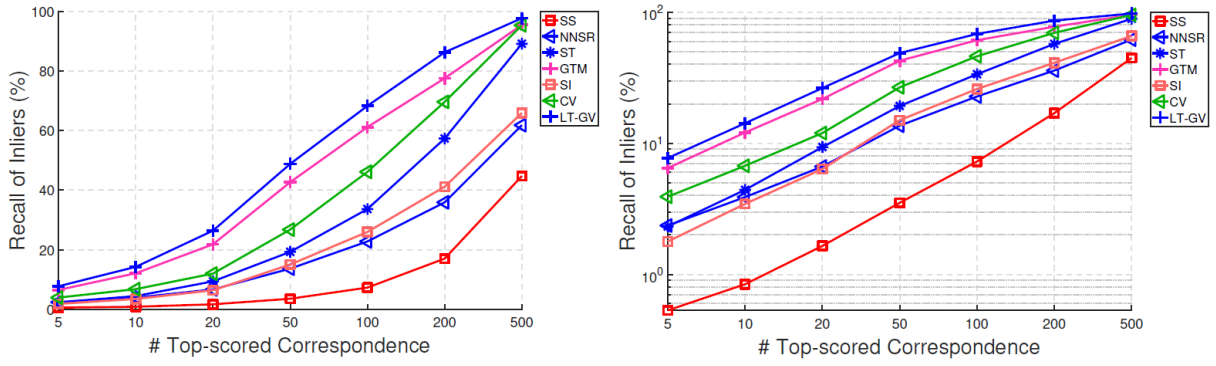

(a) U3M (linear)

(b) U3M (log)

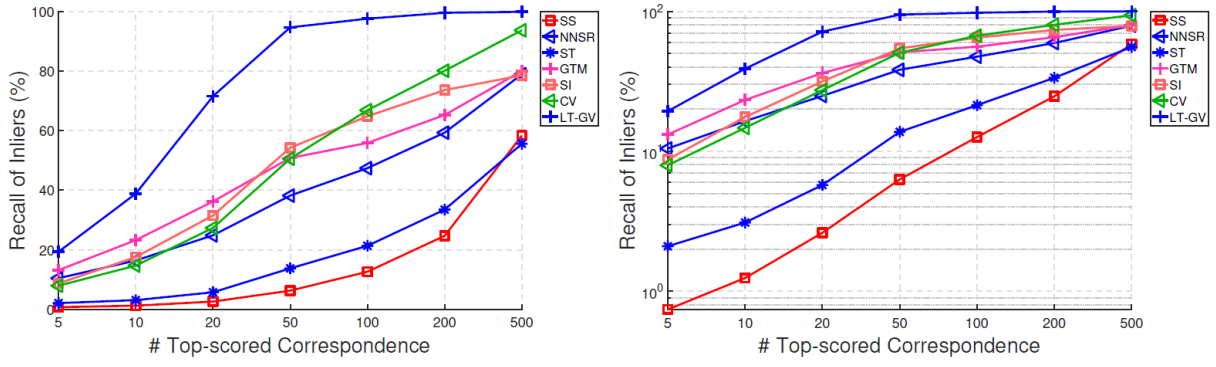

(e) U3OR (linear)

(f) U3OR (log)

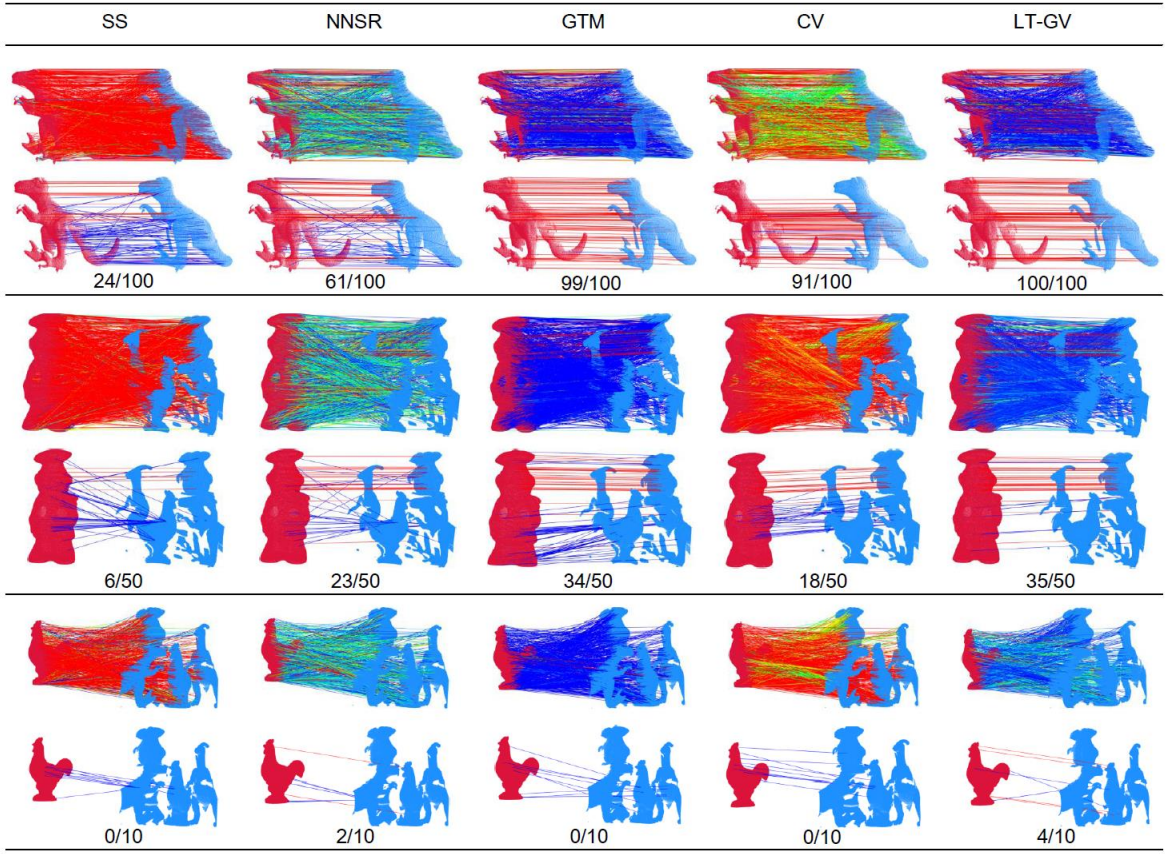

2. Our works a) Feature Matching (LT-GV)

☐ Performance: Feature matching (Robustness)

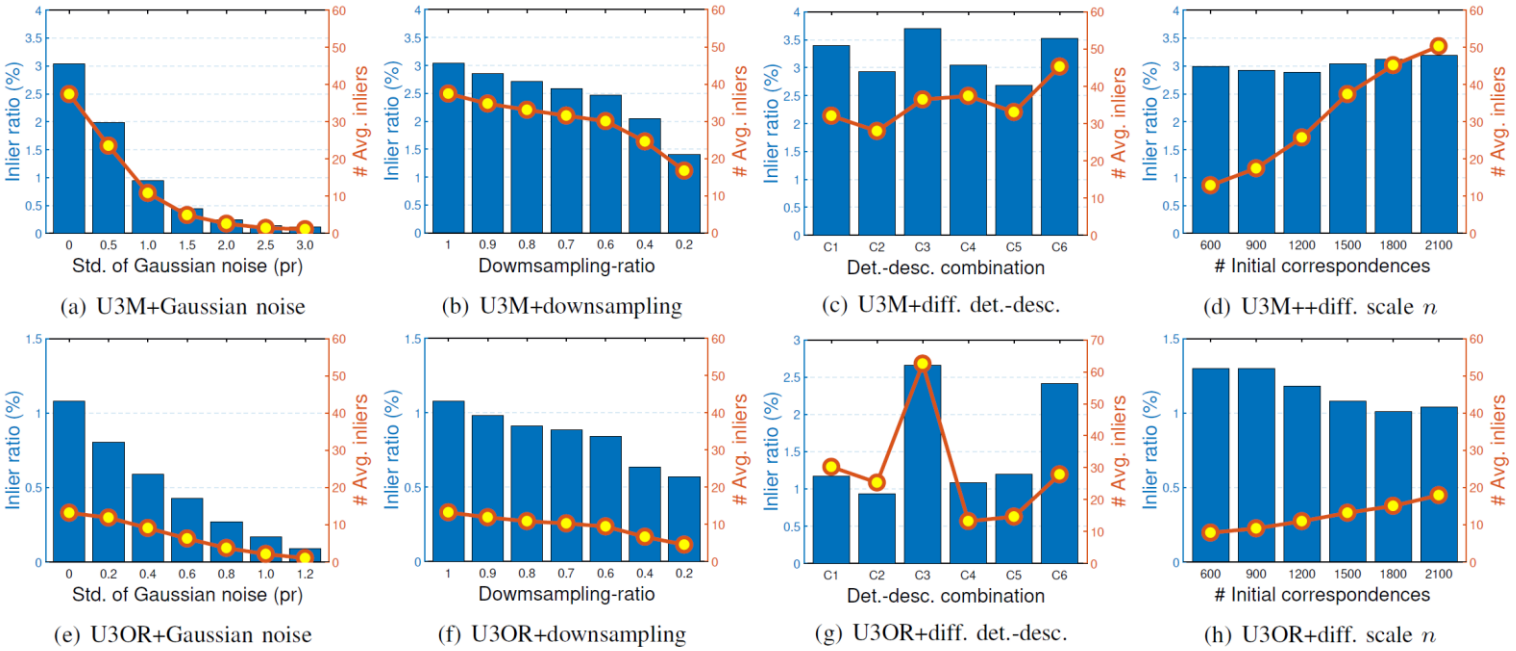

(a) U3M+Gaussian noise (b) U3M+downsampling (c) U3M+diff. det.-desc. (d) U3M++diff. scale n

(e) U3OR+Gaussian noise (f) U3OR+downsampling (g) U3OR+diff. det.-desc. (h) U3OR+diff. scale n

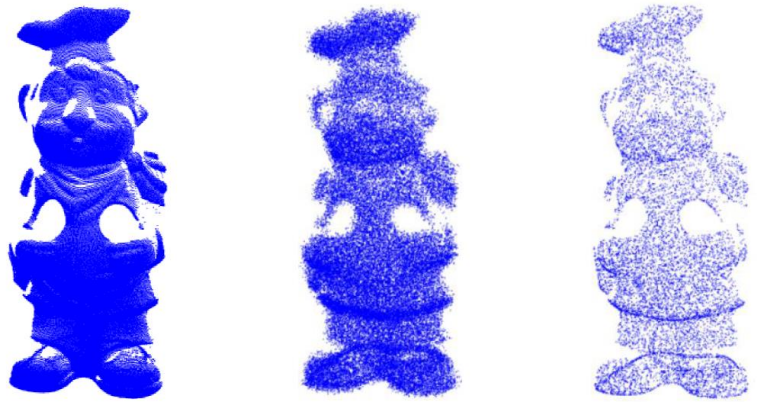

(a) clean (b) noisy (c) down-sampled

Fig. 10. Sample views of (a) a clean point cloud and point clouds with (b) 3.0 pr Gaussian noise and 90% data decimation.

2. Our works a) Feature Matching (LT-GV)

☐ Performance: Feature matching (Robustness)

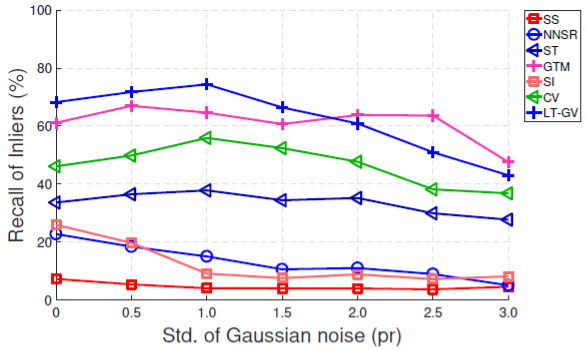

(a) Noise on U3M

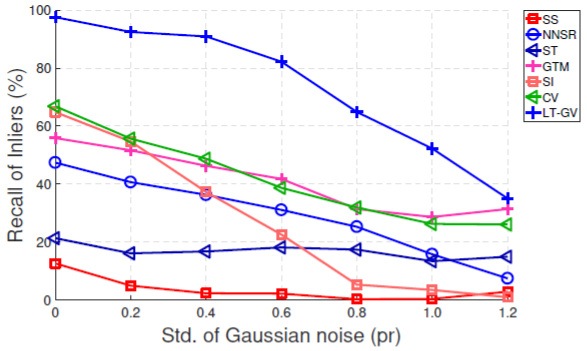

(b) Noise on U3OR

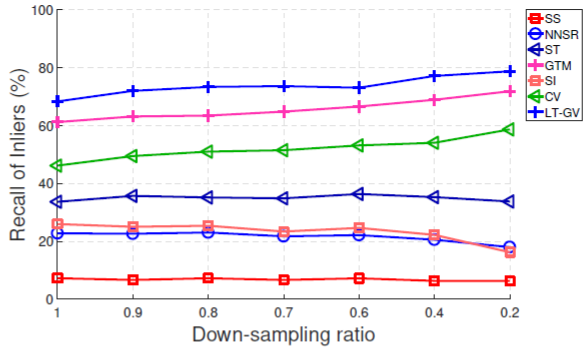

(c) Density variation on U3M

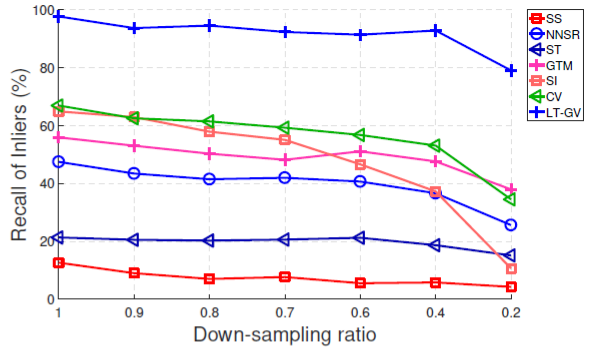

(d) Density variation on U3OR

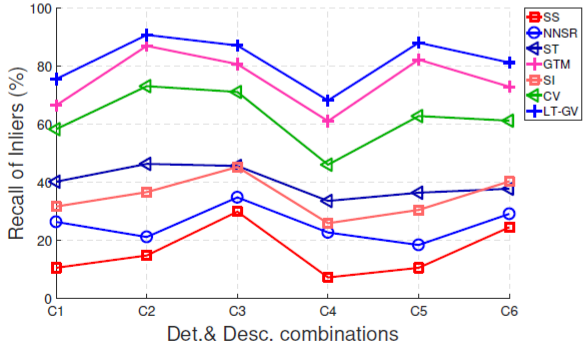

(e) Varying det.-desc. on U3M

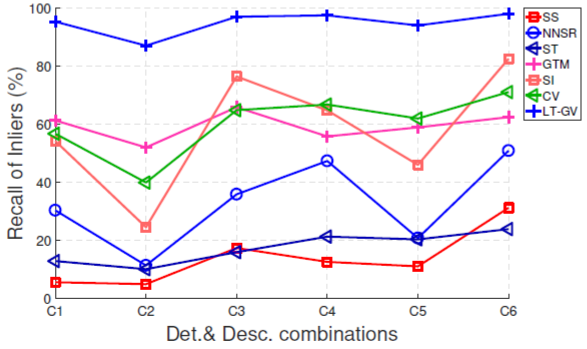

(f) Varying det.-desc. on U3OR

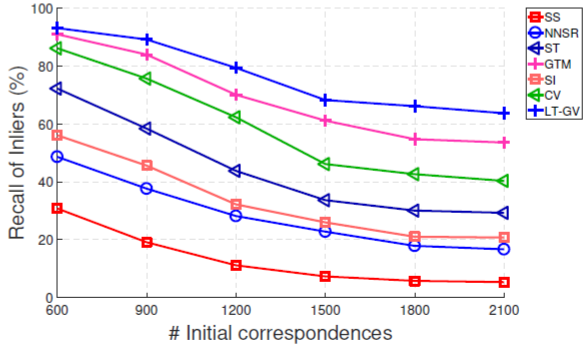

(g) Varying input scales on U3M

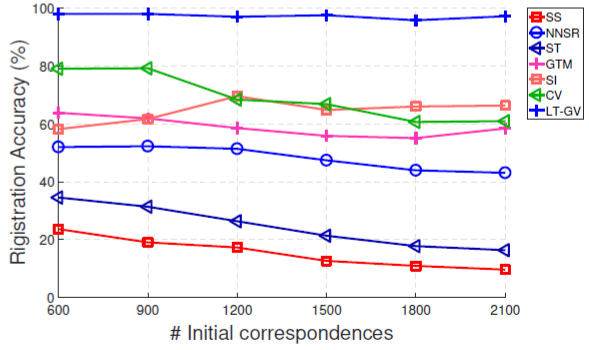

(h) Varying input scales on U3OR

2. Our works a) Feature Matching (LT-GV)

☐ Performance: Registration (input for RANSAC)

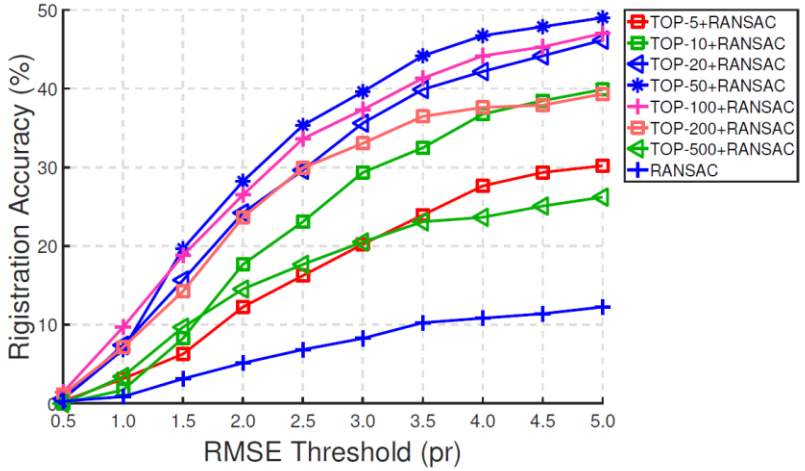

(a) U3M

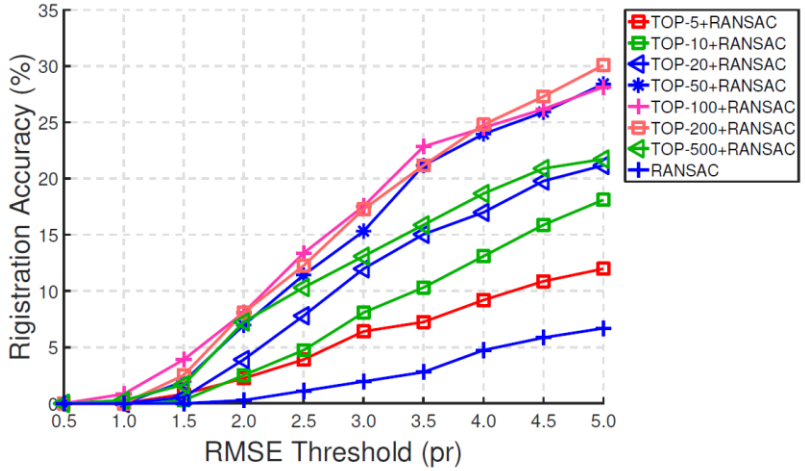

(b) BMR

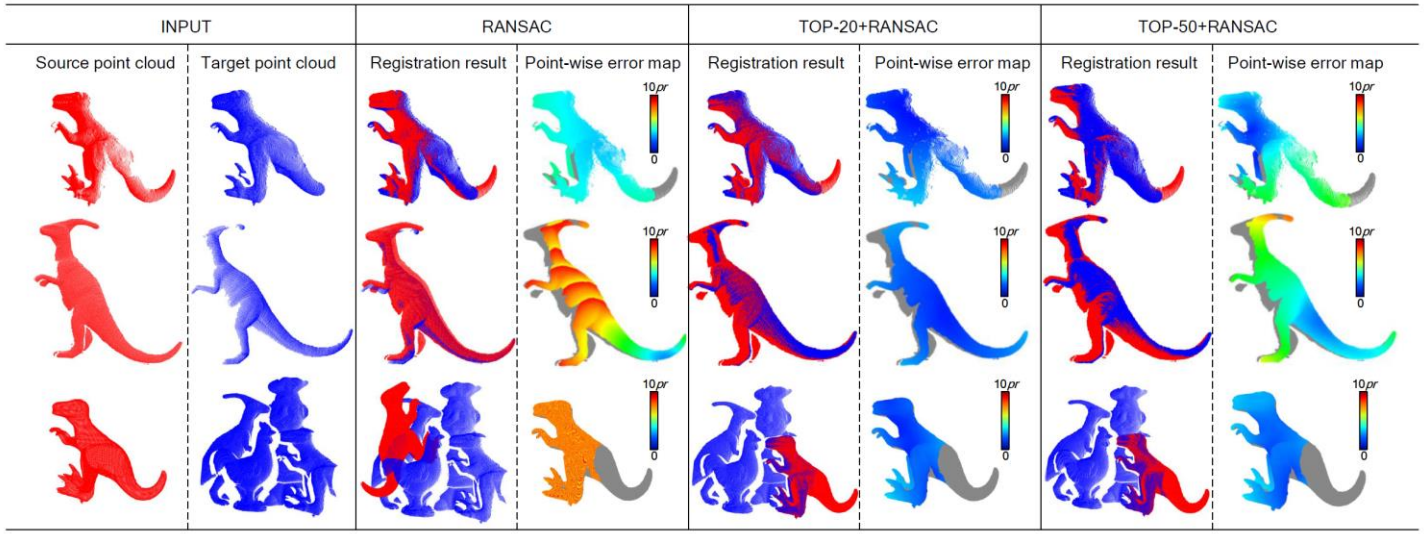

2. Our works a) Feature Matching (LT-GV)

☐ Performance: Registration (comparison with learned ones)

TABLE III
REGISTRATION RECALL PERFORMANCE (%) ON THE 3DMATCH DATASET ('–' DENOTES UNAVAILABLE BENCHMARK RECORD).

	Kitchen	Home 1	Home 2	Hotel 1	Hotel 2	Hotel 3	Study Room	MIT Lab	Avg.
(i) Traditional									
Spectral Matching [13]	–	–	–	–	–	–	–	–	55.88
RANSAC (1k iters.) [11]	60.87	71.15	53.37	67.26	58.65	70.37	44.52	51.95	58.60
RANSAC (10k iters.) [11]	77.08	82.69	67.31	82.30	73.08	81.48	61.99	66.23	73.75
GC-RANSAC (100k iters.) [17]	–	–	–	–	–	–	–	–	67.65
FGR [64]	44.07	51.28	37.98	46.90	38.46	48.15	26.71	46.75	41.16
GORE [65]	78.06	80.12	66.34	86.54	**75.96**	**83.30**	66.09	59.74	74.79
(ii) Deep learned									
3DRegNet [45]	–	–	–	–	–	–	–	–	26.31
DGR [44]	69.17	74.36	57.69	68.58	65.38	74.07	56.16	55.84	65.19
PointDSC [46]	78.26	77.56	64.90	84.07	68.27	75.93	62.33	57.14	72.70
Ours	**79.84**	**83.33**	**68.75**	**87.61**	74.04	81.48	**66.10**	**67.53**	**76.46**

TABLE IV
REGISTRATION RECALL PERFORMANCE (%) ON THE 3DLOMATCH DATASET.

	Kitchen	Home 1	Home 2	Hotel 1	Hotel 2	Hotel 3	Study Room	MIT Lab	Avg.
(i) Traditional									
RANSAC (1k iters.) [11]	10.29	9.34	16.96	17.43	12.03	32.65	2.92	4.17	11.40
RANSAC (10k iters.) [11]	23.24	15.92	27.83	25.69	18.35	38.78	6.25	11.11	20.16
GORE [65]	29.90	21.45	29.56	**44.95**	26.58	40.82	11.25	11.11	26.50
FGR [44]	0.38	2.77	4.78	1.83	1.27	4.08	0.42	1.39	1.74
(ii) Deep learned									
DGR [44]	19.05	14.53	20.00	37.61	24.05	34.69	8.33	**13.89**	19.93
PointDSC [46]	24.19	19.03	29.57	41.74	18.35	36.73	6.67	12.50	23.19
Ours	**30.86**	**22.49**	**31.74**	42.66	**28.48**	**46.94**	**12.08**	12.50	**28.02**

2. Our works b) Pose estimator

- **RANSAC eval. (IEEE/CAA JAS 2022): RANSACs are still competitive**

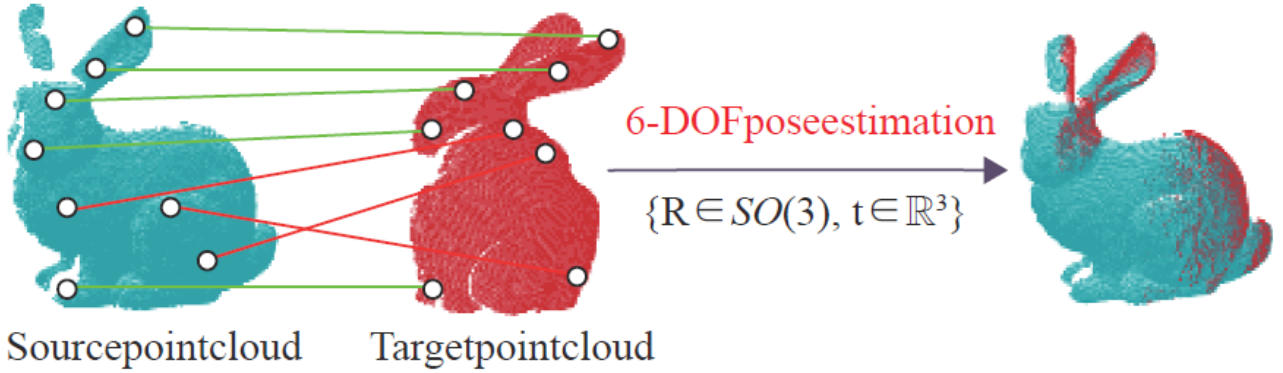

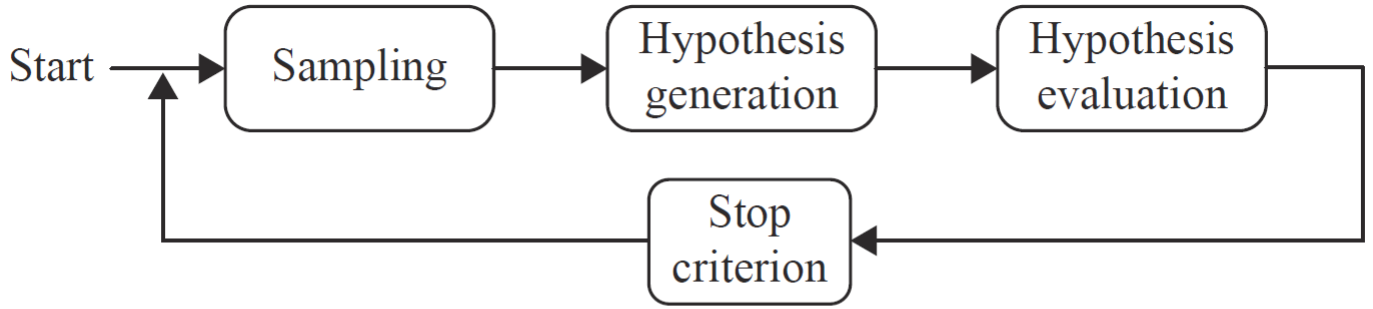

Fig. 2. The general pipeline of 6-DoF pose estimators in the RANSAC family.

2. Our works b) Pose estimator

- SAC-COT(IEEE TGRS 2021): A RANSAC variant with guided sampling

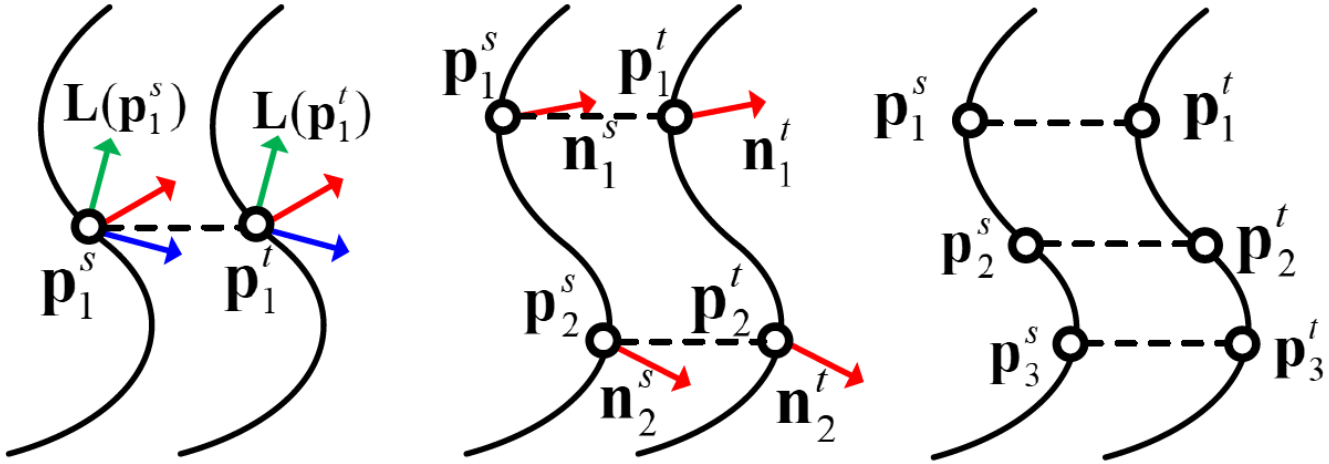

(a) 1C (b) 2C (c) 3C

Fig. 3. A 6-DoF pose hypothesis can be generated with one (1C), two (2C), or three (3C) correspondences. Here, $\mathbf{p}$, $\mathbf{n}$, and $\mathbf{L}$ denote a 3D keypoint, a normal vector, and an LRF, respectively.

2. Our works b) Pose estimator

SAC-COT(IEEE TGRS 2021): A RANSAC variant with guided sampling

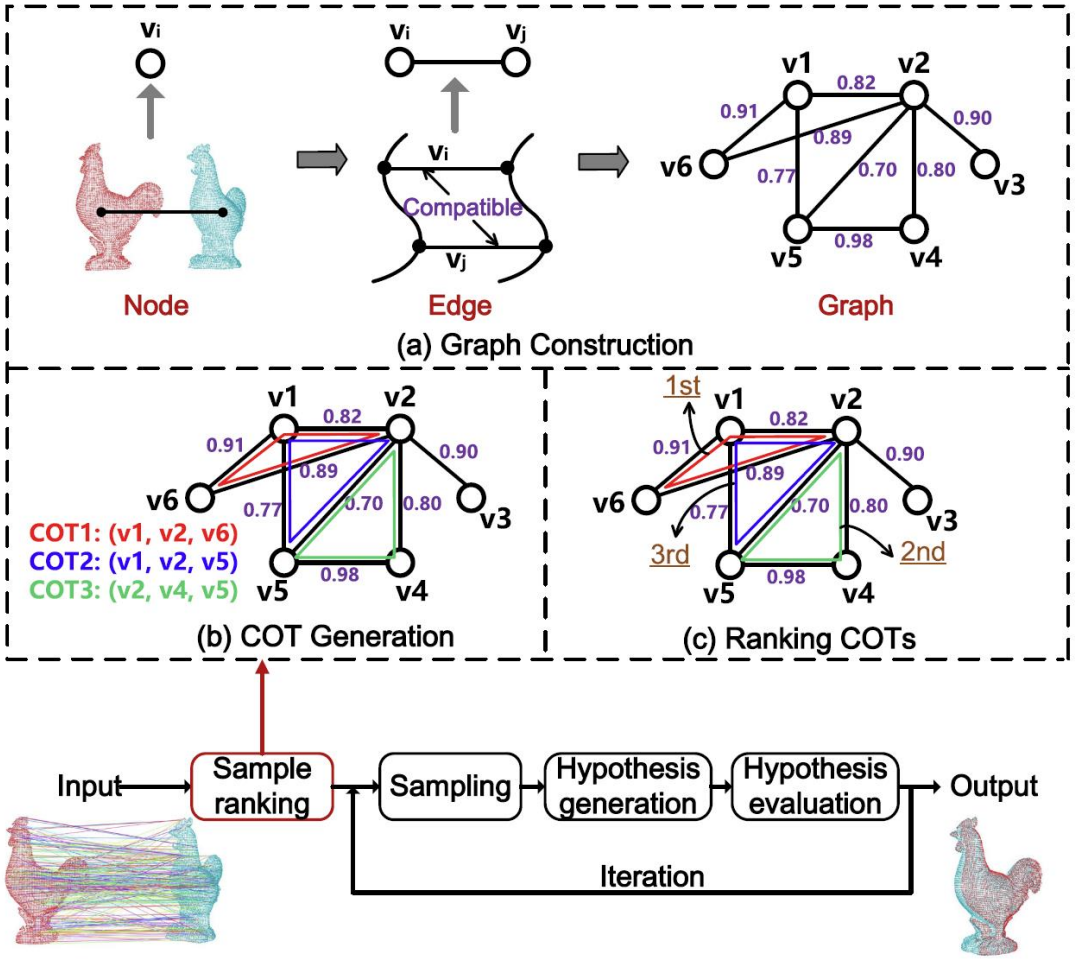

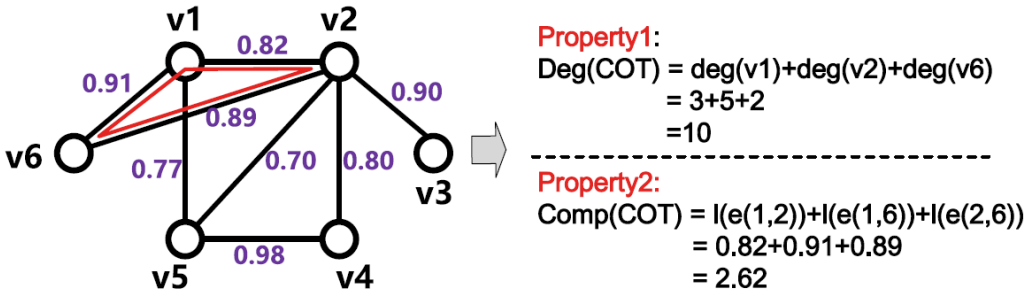

Fig. 4. Illustration of two properties defined for a COT ($\deg(v_i)$: degree of node v_i and $l(e(i, j))$: compatibility score of edge $e(i, j)$).

2. Our works b) Pose estimator

☐ Performance: comparison with RANSAC

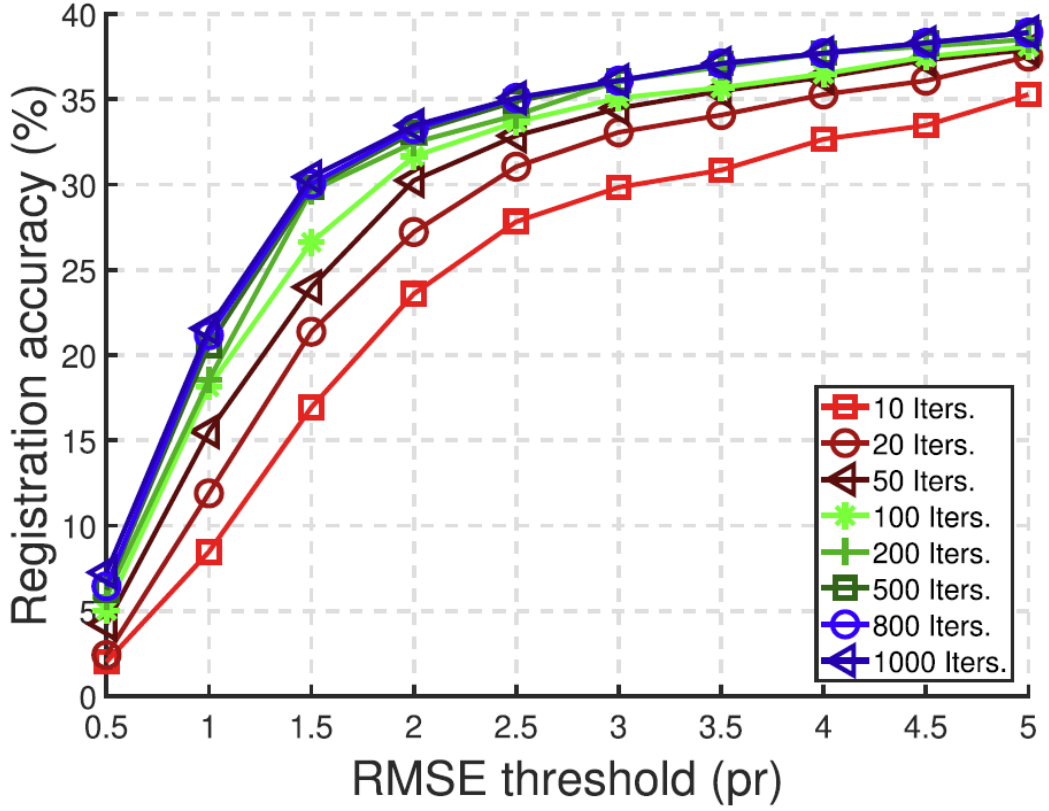

(a)

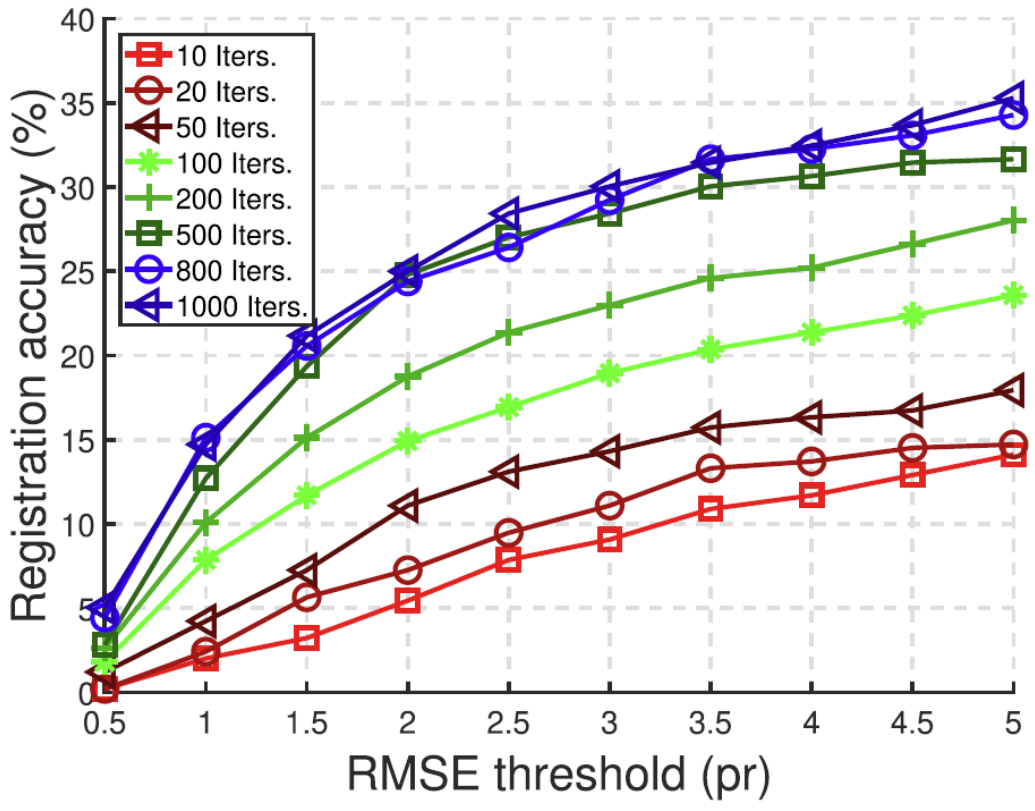

(b)

2. Our works b) Pose estimator

☐ Performance: comparison with RANSAC

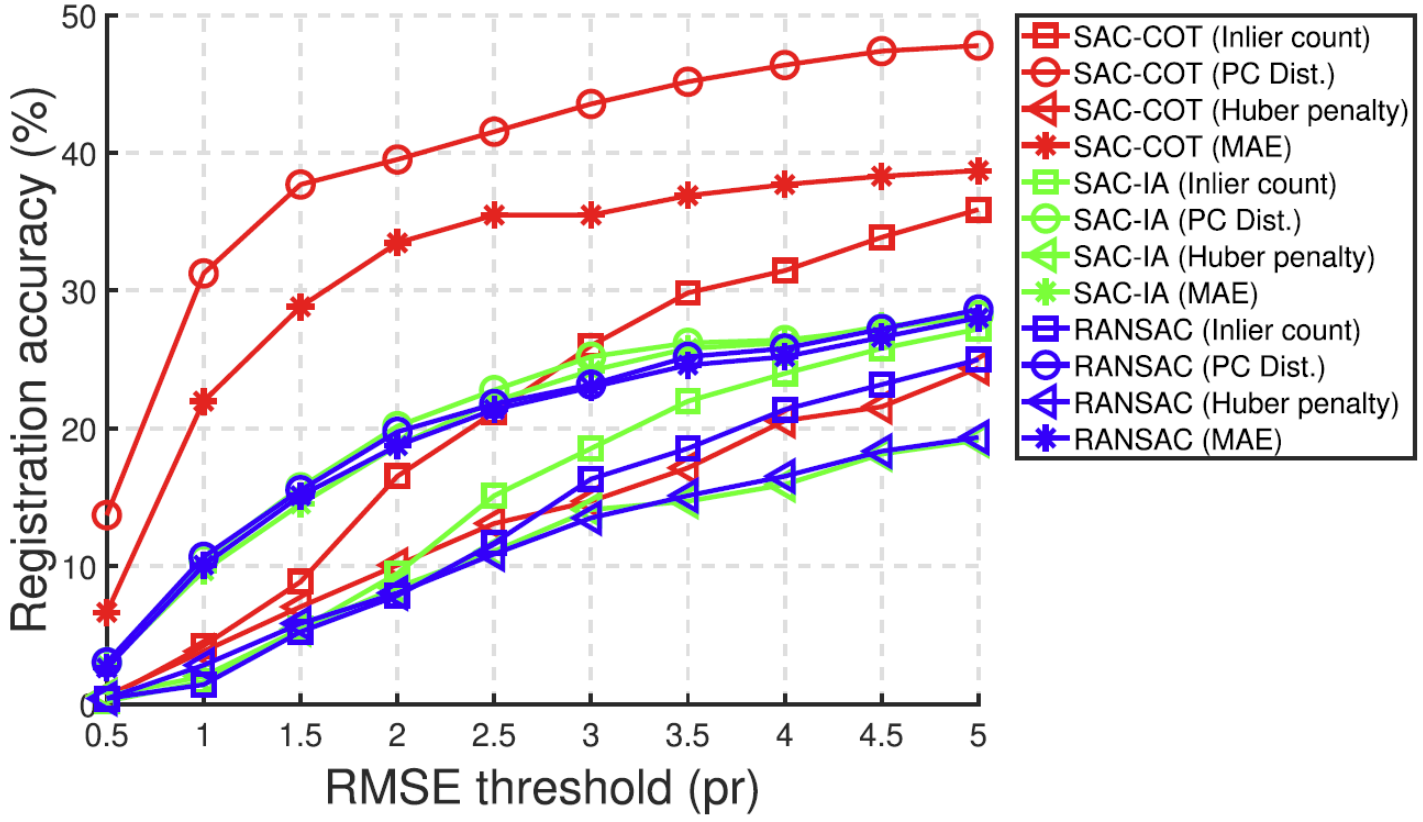

Fig. 12. Comparison of SAC-COT with SAC-IA and RANSAC when using four different hypothesis evaluation metrics. The objective is to show that our COT-based guided sampling method is general to different hypothesis evaluation metrics.

2. Our works b) Pose estimator

☐ Performance: comparison with other RANSAC variants

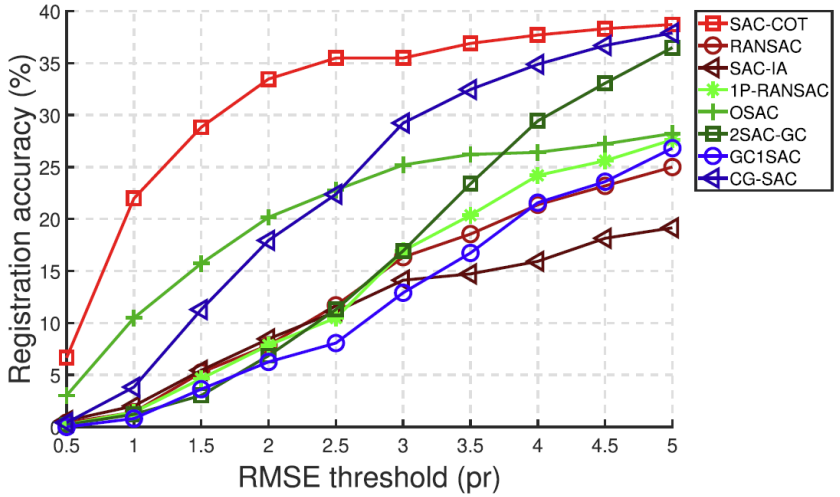

(a)

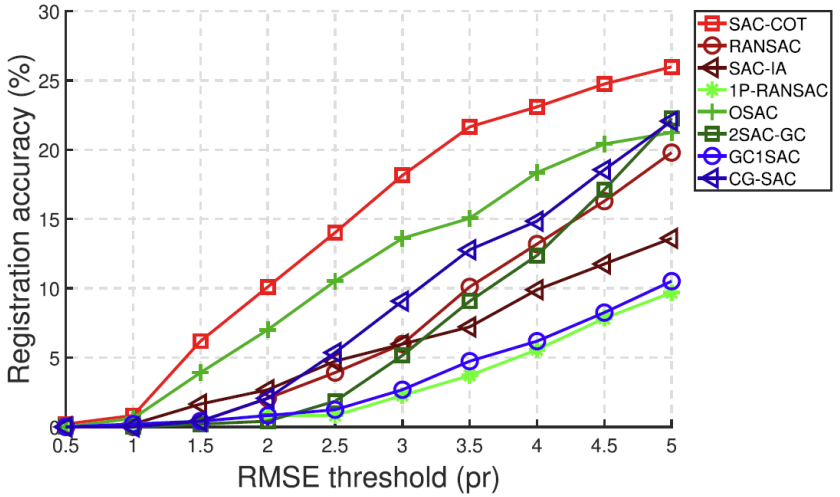

(b)

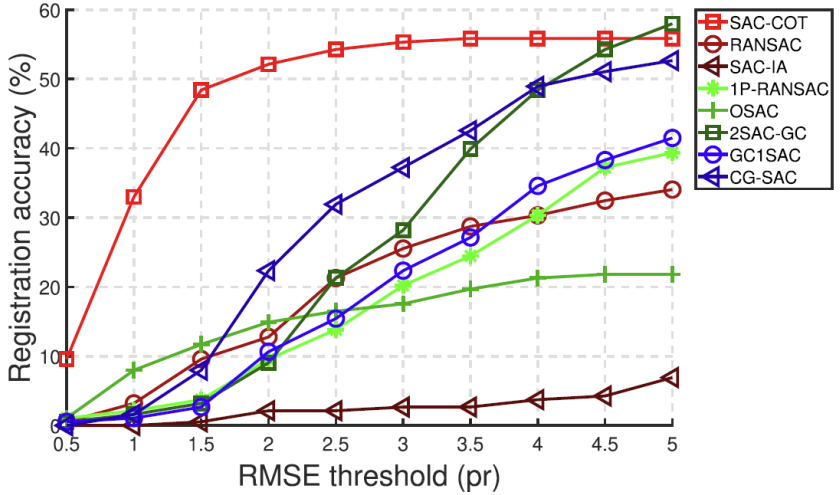

(c)

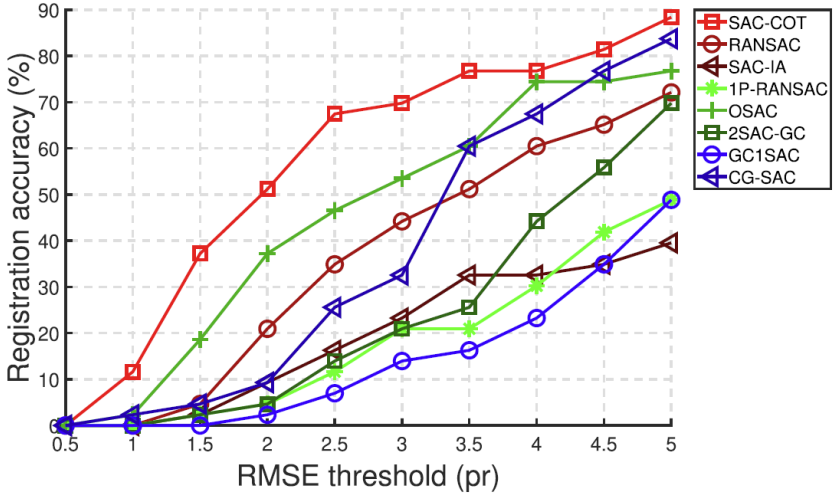

(d)

2. Our works b) Pose estimator

☐ Performance: robustness

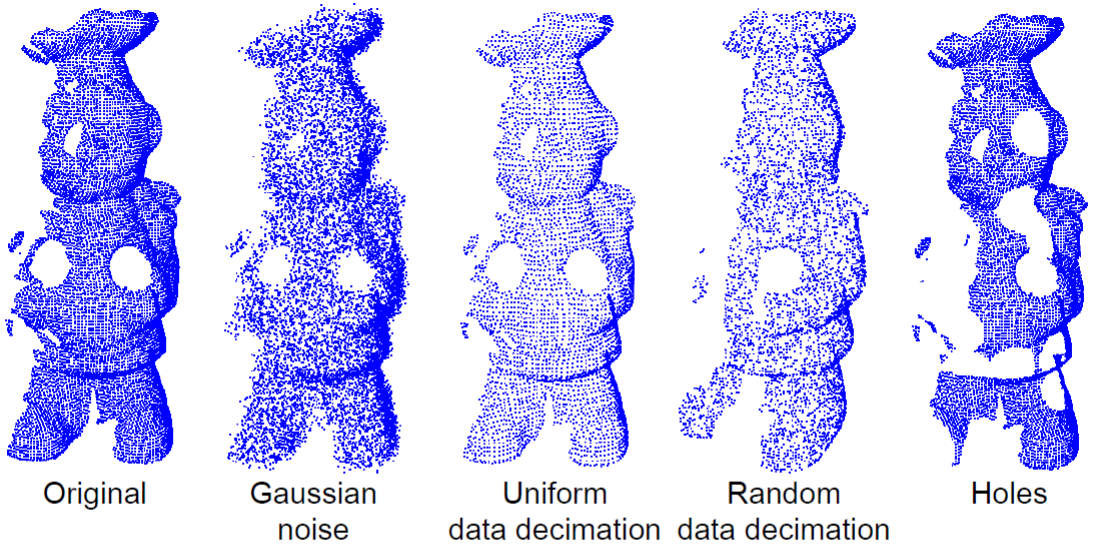

Fig. 7. Visualization of point clouds with different nuisances. From left to right: noise-free point cloud and point clouds with 1.5 pr Gaussian noise, 60% uniform data decimation, 60% random data decimation, and 14 holes, respectively.

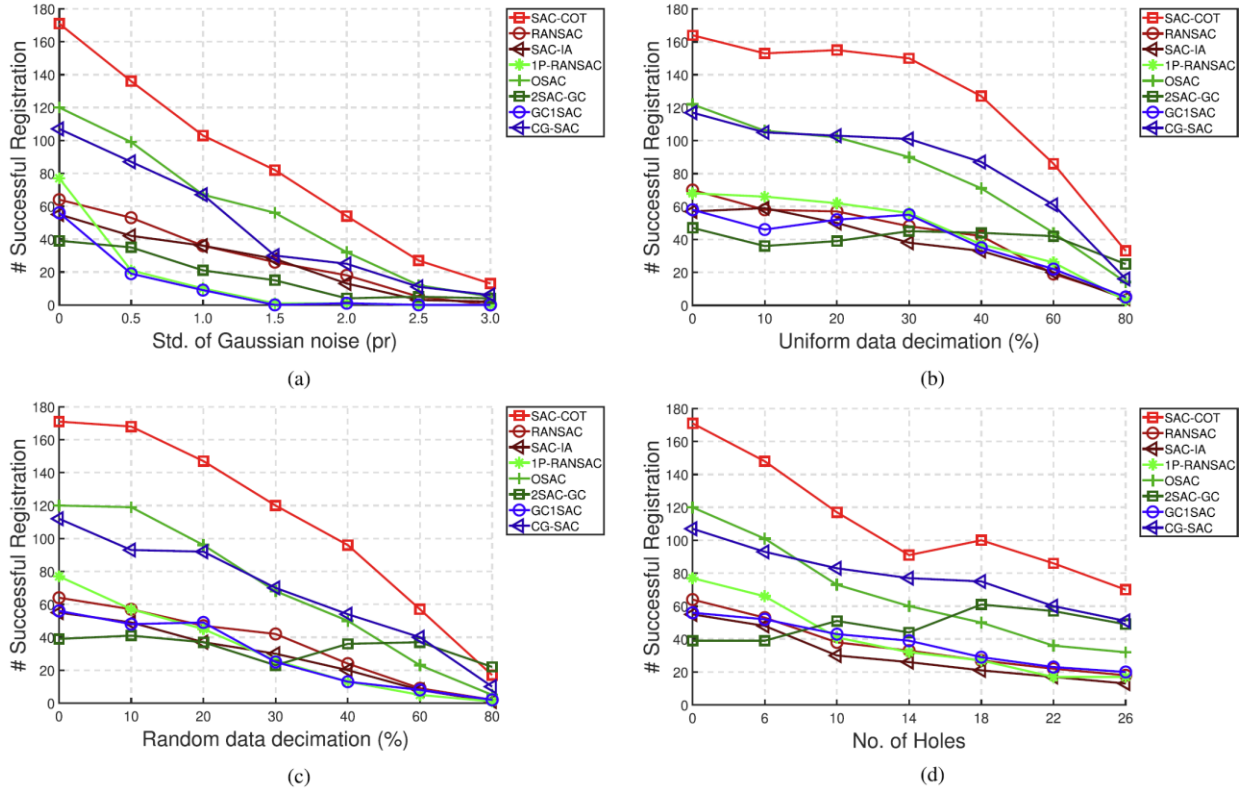

2. Our works b) Pose estimator

☐ Performance: <5% inlier ratio case

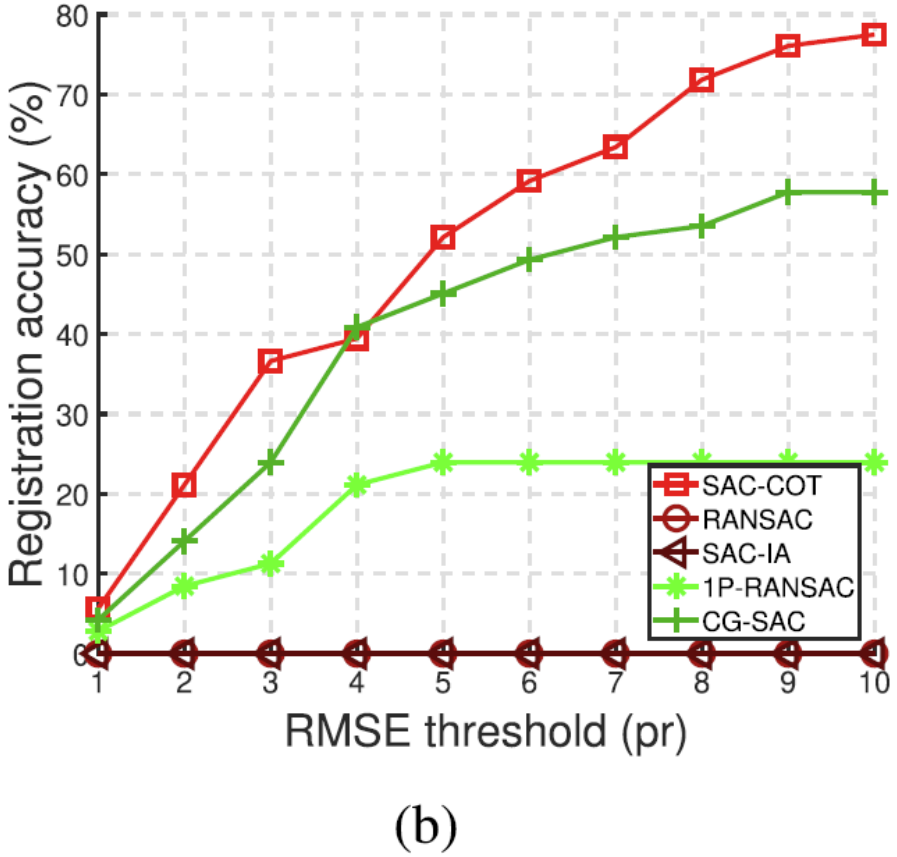

(b)

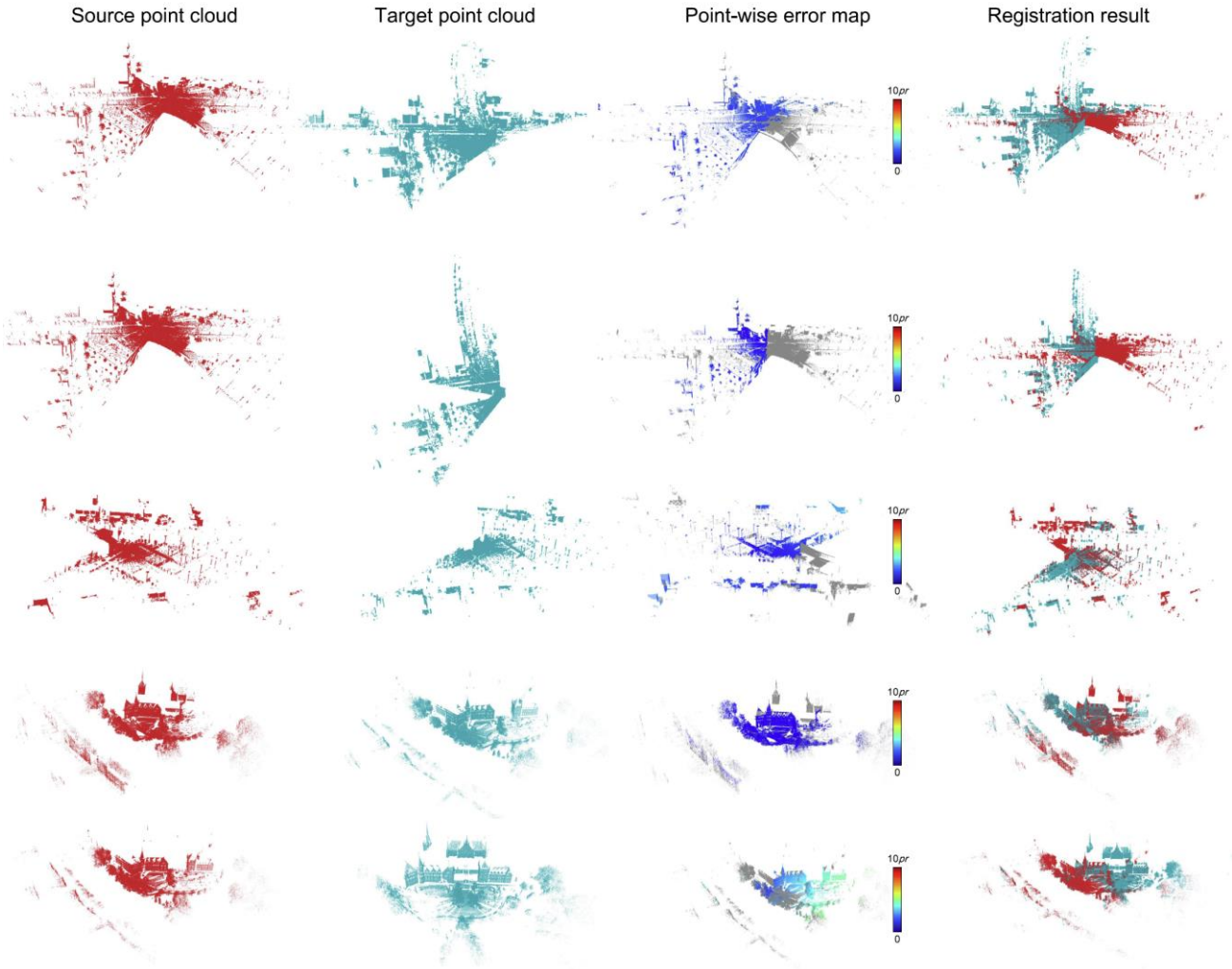

2. Our works b) Pose estimator

- **RANSAC metrics (IEEE TCSVT 2021): Efficient and Robust hypothesis evaluation metrics**

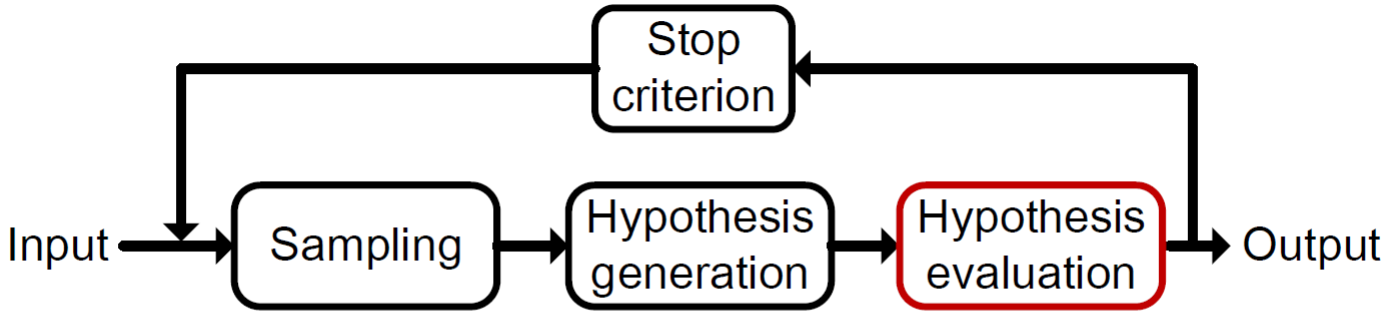

Fig. 1. The general pipeline of RANSAC for 6-DoF pose estimation.

- **Not all inliers are equal**

2. Our works b) Pose estimator

☐ RANSAC metrics (IEEE TCSVT 2021): Efficient and Robust hypothesis evaluation metrics

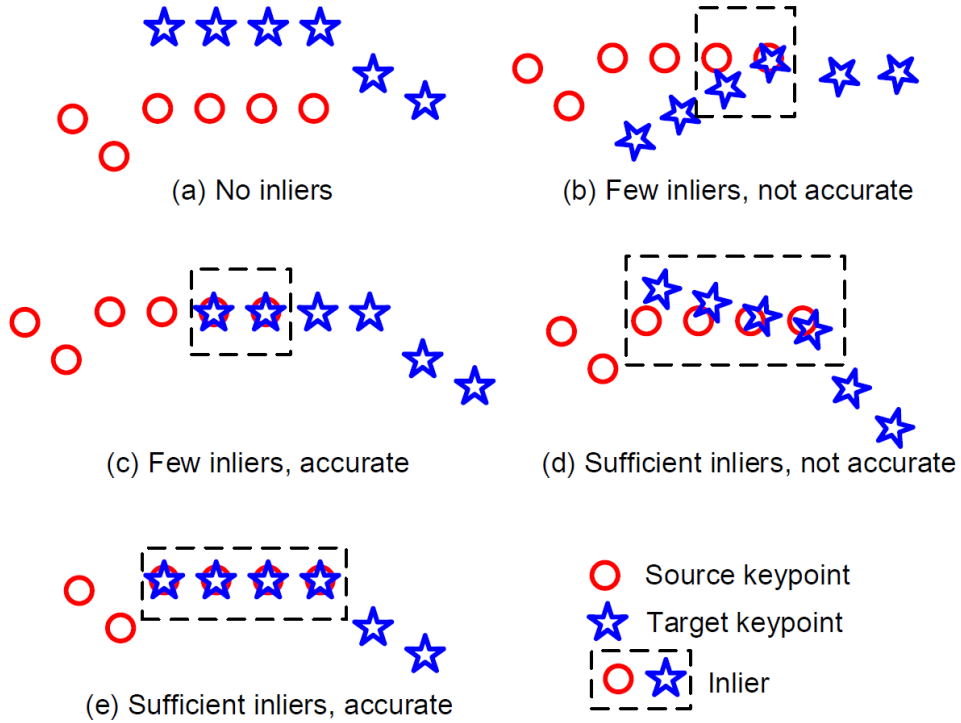

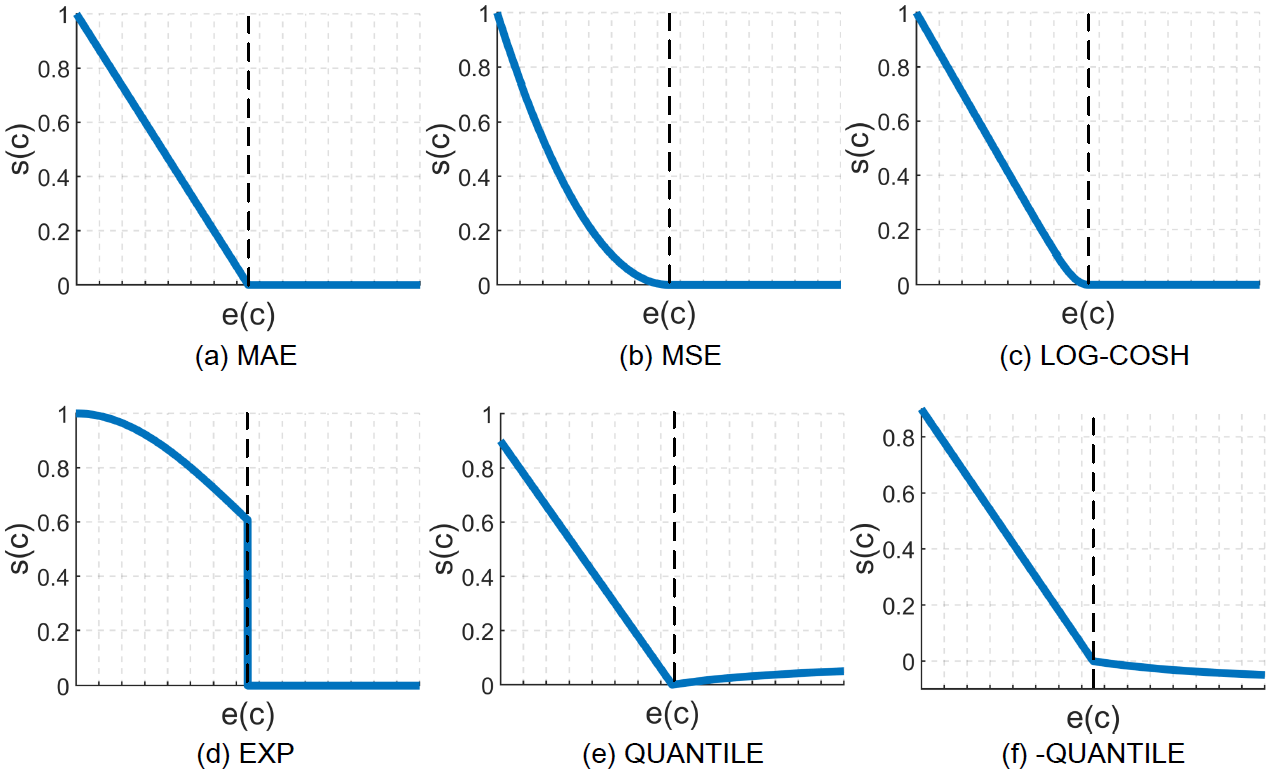

Fig. 2. Five typical cases for RANSAC hypothesis evaluation.

2. Our works b) Pose estimator

☐ Performance: Varying iterations

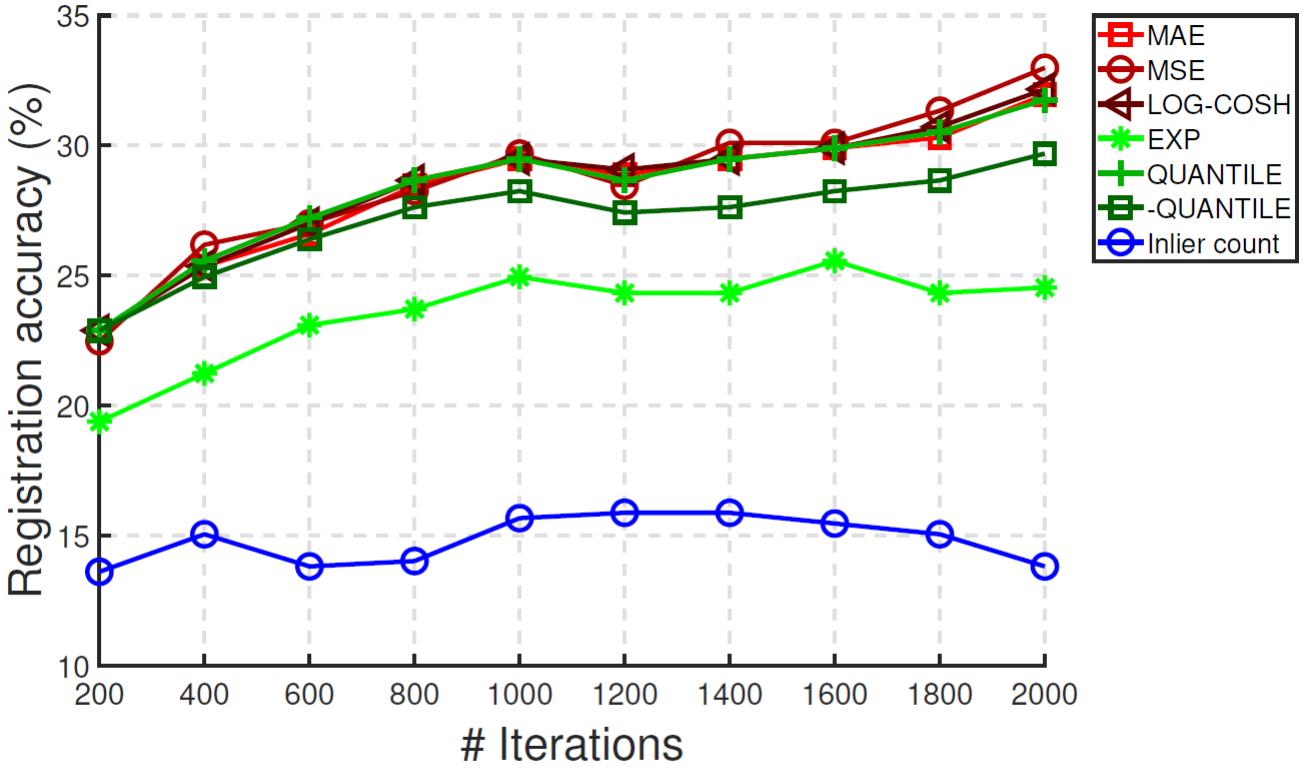

Fig. 6. The effects of varying the number of iterations on registration accuracy (tested on the U3M dataset).

2. Our works b) Pose estimator

☐ Performance: Sensitivity to inlier determining threshold

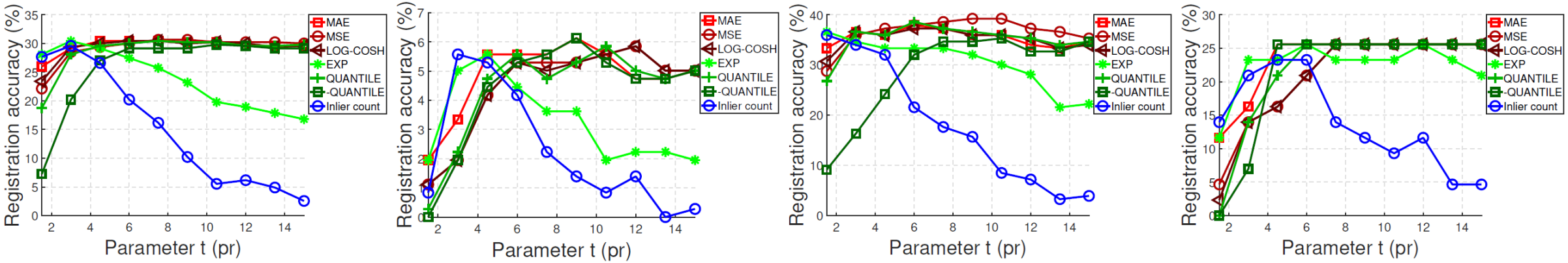

(a) U3M (b) BMR (c) U3OR (d) BoD5

2. Our works b) Pose estimator

☐ Performance: Scene registration results

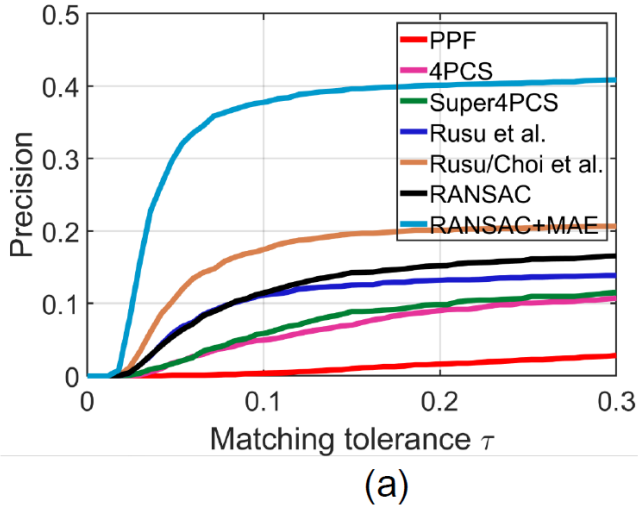

(a)

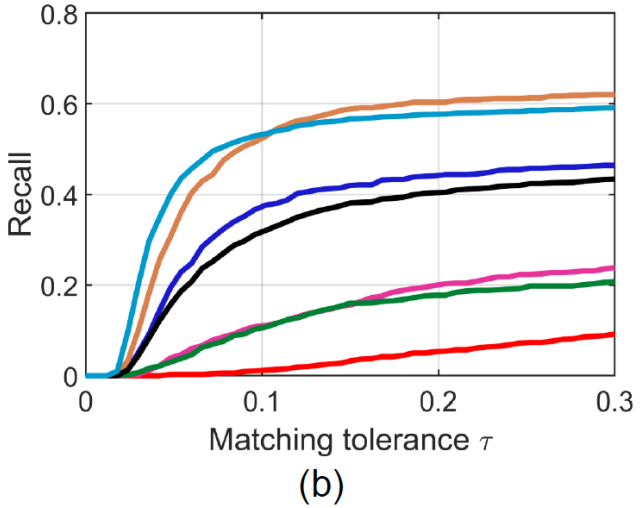

(b)

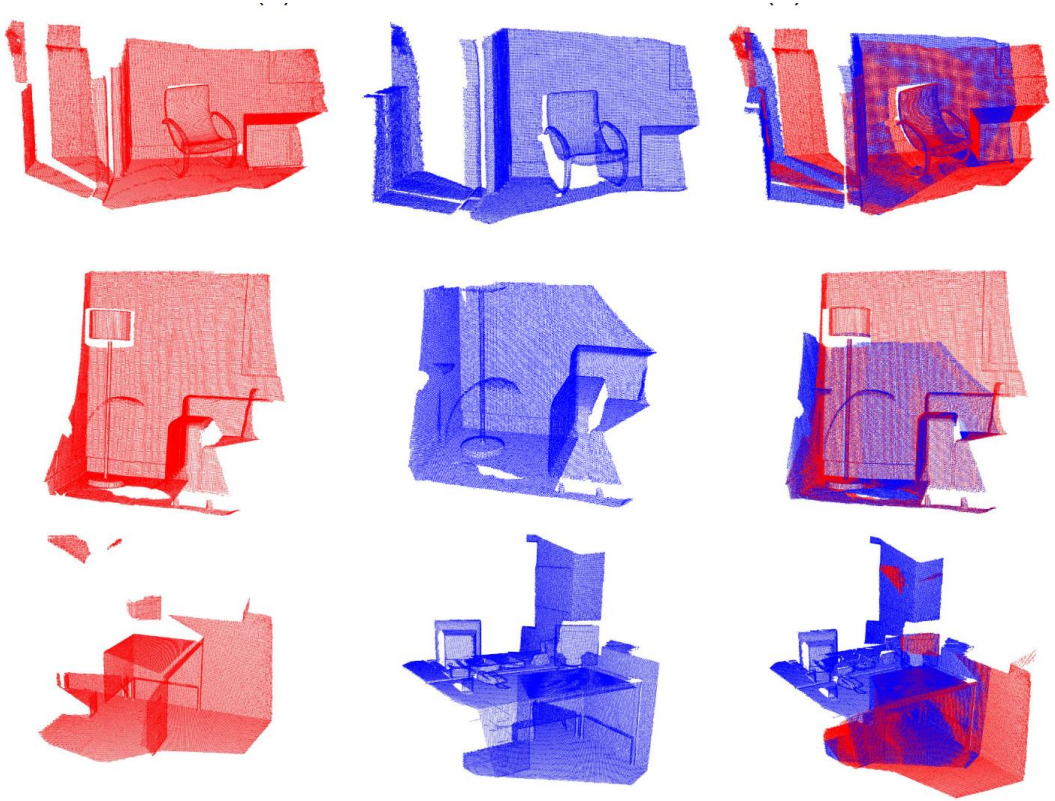

3. Summary

- Geometric methods still hold great potential for 3D point cloud registration
- RANSAC, a 1981 estimator, is still active and can be further improved for 3D point cloud registration
- In national defense 3D reconstruction applications, geometric-only methods are arguably more reliable choices
- In the deep learning era, more attention on geometric methods is deserved.

Thank you!

END

jqyang@nwpu.edu.cn
https://sites.google.com/view/jiaqiyang